FORCE CONTROL OF REDUNDANT ROBOTS IN UNSTRUCTURED ENVIRONMENT

Bojan Nemec (non-memmber) and Leon Žlajpah (non-memmber)

Jožef Stefan Institute

Jamova 39, 1000 Ljubljana, Slovenia

Fax : +386 1 423 22 09

E-mail: bojan.nemec@ijs.si

ABSTRACT: In the paper a method for force control of redundant robots in unstructured environment is proposed. We assume that the obstacles are not known in advance. Hence, the robot arm has to be compliant with the environment while tracking the desired position and force at the end effector. First, the dynamic properties of the internal motion of redundant manipulators are considered. The motion is decoupled into the end-effector motion and the internal motion. Next, the dynamic model of a redundant manipulator is derived. Special attention is given to the inertial properties of the system in the space where internal motion is taking place; we define a *null space effective inertia* and its inverse. Finally, a control method is proposed which completely decouples the motion of the manipulator into the task space motion and the internal motion, and enables the selection of dynamic characteristics in both subspaces separately. The proposed method is verified with the simulation and with the experimental results of 4.D.O.F planar redundant robot

KEYWORDS: Robot dynamics, Compliance control, Redundant systems

1. INTRODUCTION

One of the important issues of the new generation of robotic manipulators is kinematic redundancy. Kinematic redundancy is characterized by extra degrees of freedom with respect to the given motion posed by the assigned primary task. A redundant manipulator has the ability to move the end-effector along the same task state using different configurations of the mechanical structure. This provides a means for solving sophisticated motion tasks such as avoiding obstacles, avoiding singularities, optimizing manipulability, minimizing joint torques, etc.. The result is a significant increase in the dexterity of the system, which is essential to accomplish complex tasks. On the other hand, redundancy also has an important influence on the dynamic behaviour of the robotic system. An appropriate control of dynamic properties is essential for higher performance in robotic manipulation. Most of the research in the field of the dynamics of robotic manipulators has been devoted to the dynamics in the joint space. To control the dynamic properties of the system in the joint space different control methodologies have been proposed [12, 1]. As the next step, methods have been proposed where the control takes place in the task space [13]. These methods include the transformations between joint space trajectories and task space trajectories. However, in the case of redundant manipulators these transformations are not unique. Different methodologies have been proposed to resolve the redundancy like optimization of a given performance criteria while satisfying a primary task [16].

To overcome the limitations of control methods based on the joint space dynamics methods Khatib [8] proposed a method for dealing with dynamics and control in the task space. This method enables the description, analysis and control of the robot behaviour in the task space, and can also be used for redundant manipulators when the dynamic behaviour of the end-effector is of interest. However, for the redundant manipulators the end-effector dynamics is only one part of the dynamics of the whole manipulator. The “rest” dynamics represents the dynamics of the internal motion of the manipulator. Recently, Park [17] proposed a decomposition of dynamics of kinematically redundant manipulators into the task space dynamics and null space dynamics based on a minimally reparametrized homogenous velocity.

The majority of the task posed to the robots requires interaction with the environment. Therefore, ability to control the interaction forces is essential for a modern robot. In [15] we have proposed an approach to the force control of redundant robots. However, the proposed approach

requires structured environment, where the position of the obstacles is known into advance or complex sensory system is used to detect the environment obstacles. But there are many situations where the obstacles are not known into advance or are changing position. An example of such task could be working into a tube or working in a completely dark environment, where the vision sensors can not be used. Humans solves such a situation by adapting the compliance of the arm. Our approach tries to imitate the human behaviour in such a situation. This requires the study of the dynamic properties of the internal motion of redundant manipulators. We analyze what are the causes for the internal motion and how to use the internal motion to improve the performances of the overall system. Next, the influence of the selection of pseudo or generalized inverse on the internal motion is discussed and a method to derive the model describing the dynamics of the internal motion is presented. We define a *null space effective inertia* and its inverse. Finally, impedance control method is presented which completely decouple the motion of the manipulator into the task space motion and the internal motion, and enable the selection of dynamic characteristics in both subspaces separately.

2. KINEMATICS

The robotic systems under study are n degrees of freedom (DOF) serial manipulators. We consider only the redundant systems which have more DOF than needed to accomplish the task, i.e. the dimension of the joint space n exceeds the dimension of the task space m, $n > m$. Let the configuration of the manipulator be represented by the vector $\boldsymbol{q}$ of n joint positions, and the end-effector position (and orientation) by m-dimensional vector $\boldsymbol{x}$ of task positions (and orientations). The joint and task velocities are related by the following expression

$$\dot{\boldsymbol{x}} = \mathbf{J}\dot{\boldsymbol{q}} \tag{1}$$

where $\mathbf{J}$ is the $m \times n$ manipulator Jacobian matrix. Mapping of joint velocities to the task velocities is unique, while mapping of the task velocities to the joint velocities is not. The general solution of Eq. (1) can be given as

$$\dot{\boldsymbol{q}} = \mathbf{J}^{\#}\dot{\boldsymbol{x}} + \mathbf{N}\dot{\boldsymbol{q}} \tag{2}$$

where $\mathbf{J}^{\#}$ is the generalized inverse of $\mathbf{J}$ and $\mathbf{N}$ is $n \times n$ matrix representing the projection of $\dot{\boldsymbol{q}}$ into the null space of $\mathbf{J}$, $\mathbf{N} = (\mathbf{I} - \mathbf{J}^{\#}\mathbf{J})$. The first term on the right side of Eq. (2) represents the part of the joint space velocity necessary to perform the task and is denoted as $\dot{\boldsymbol{q}}_x$, $\dot{\boldsymbol{q}}_x = \mathbf{J}^{\#}\dot{\boldsymbol{x}}$.

The second term denoted as $\dot{\boldsymbol{q}}_n$, $\dot{\boldsymbol{q}}_n = \mathbf{N}\dot{\boldsymbol{q}}$, represents the joint space velocity due to the internal motion. Actually, $\dot{\boldsymbol{q}}$ in the second term of Eq. 2 can be an arbitrary velocity vector and is usually used to perform an additional subtask like optimization of different cost functions, obstacle avoidance, etc.

Differentiating Eq. (1), we obtain the relation between joint space accelerations and task space accelerations

$$\ddot{\boldsymbol{x}} = \mathbf{J}\ddot{\boldsymbol{q}} + \dot{\mathbf{J}}\dot{\boldsymbol{q}} \tag{3}$$

Considering also the accelerations in the null space of $\mathbf{J}$ the general solution of Eq. (3) is typically given in the form

$$\ddot{\boldsymbol{q}} = \mathbf{J}^{\#}(\ddot{\boldsymbol{x}} - \dot{\mathbf{J}}\dot{\boldsymbol{q}}) + \mathbf{N}\ddot{\boldsymbol{q}} \tag{4}$$

To be able to decompose the joint accelerations $\ddot{\boldsymbol{q}}$ into accelerations subjected to the task space motion and to the internal motion Eq. (4) has to be rewritten into the form

$$\ddot{\boldsymbol{q}} = \mathbf{J}^{\#}\ddot{\boldsymbol{x}} + \dot{\mathbf{J}}^{\#}\dot{\boldsymbol{x}} + \mathbf{N}\ddot{\boldsymbol{q}} + \dot{\mathbf{N}}\dot{\boldsymbol{q}} \tag{5}$$

The above equation can also be obtained by differentiating (2). The first two terms on the right side of Eq. (5) represent the joint space acceleration due to the task space motion, and last two terms represent the joint space acceleration due to the internal motion. The terms $\dot{\mathbf{J}}^{\#}\dot{\boldsymbol{x}}$ and $\dot{\mathbf{N}}\dot{\boldsymbol{q}}$ describe the accelerations due to the change in the configuration of the manipulator and are required to maintain the task space and null space velocity, respectively [14].

Similar decomposition exists also for the forces. For redundant manipulators the relationship between the m-dimensional generalized force in task space $\boldsymbol{F}$ including linear forces and torques and the corresponding n-dimensional generalized joint space force $\boldsymbol{\tau}$ is described by

$$\boldsymbol{\tau} = \mathbf{J}^T\boldsymbol{F} + \mathbf{N}^T\boldsymbol{\tau} \tag{6}$$

where $\mathbf{N}^T$ is $n \times n$ matrix representing the projection into the null space of $\mathbf{J}^T$.

3. SELECTION OF THE GENERALIZED INVERSE

There is an infinite number of the generalised inverses $\mathbf{J}^{\#}$, which satisfy the equation

$$\mathbf{J}\mathbf{J}^{\#}\mathbf{J} = \mathbf{J} \tag{7}$$

In the past the Moore-Penrose pseudoinverse [10] has been widely used to resolve the redundancy. It is defined as

$$\mathbf{J}^{+} = \mathbf{J}^{T}(\mathbf{J}\mathbf{J}^{T})^{-1}$$

where $n > m$. Its "weighted" counterpart [6] is defined as

$$\mathbf{J}_{w}^{+} = \mathbf{W}^{-1}\mathbf{J}^{T}(\mathbf{J}\mathbf{W}^{-1}\mathbf{J}^{T})^{-1}$$

where $\mathbf{W}$ is an $n \times n$ weighting matrix. A special form of $\mathbf{J}_{w}^{+}$ is when $\mathbf{W} = \mathbf{H}$, where $\mathbf{H}$ is the inertia matrix of the manipulator. Khatib [9] has proven that

$$\bar{\mathbf{J}} = \mathbf{H}^{-1}\mathbf{J}^{T}(\mathbf{J}\mathbf{H}^{-1}\mathbf{J}^{T})^{-1} \tag{8}$$

is the only pseudoinverse which is dynamically consistent, i.e. the task space acceleration $\ddot{\boldsymbol{x}}$ is not affected by any arbitrary torques $\boldsymbol{\tau}_n$ applied through the associated null space, $\bar{\mathbf{N}}^{T}\boldsymbol{\tau}_n$, $\bar{\mathbf{N}}^{T} = (\mathbf{I} - \mathbf{J}^{T}\bar{\mathbf{J}}^{T})$. $\bar{\mathbf{N}}$ denotes the projection of the $\boldsymbol{\tau}$ into the null space of $\mathbf{J}^{T}$ using the inertia weighted pseudoinverse $\bar{\mathbf{J}}$. Additionally, the dynamically consistent generalized inverse $\bar{\mathbf{J}}$ is the only generalized inverse which assures that an external force does not produce a null space acceleration [5].

4. MANIPULATOR DYNAMICS

Assuming the manipulator consists of rigid bodies the joint space equations of motion can be written in a form

$$\boldsymbol{\tau} = \mathbf{H}(\boldsymbol{q})\ddot{\boldsymbol{q}} + \mathbf{C}(\boldsymbol{q},\dot{\boldsymbol{q}})\dot{\boldsymbol{q}} + \mathbf{g}(\boldsymbol{q}) - \boldsymbol{\tau}_E \tag{9}$$

where $\boldsymbol{\tau}$ is the n-dimensional vector of control torques, $\mathbf{H}$ is the $n \times n$ symmetric positive-definite inertia matrix, $\mathbf{C}(\boldsymbol{q},\dot{\boldsymbol{q}})$ is the $n \times n$ matrix due to the Coriolis and centrifugal forces, and $\mathbf{g}$ is the n-dimensional vector of gravity forces. Vector $\boldsymbol{\tau}_E$ summarizes effects of all external forces acting on the manipulator.

Using the relation $\mathbf{I} = \mathbf{J}^{T}\mathbf{J}^{\#T} + \mathbf{N}^{T}$ and substituting Eqs. (4) and (6) into Eq. (9), the model (9) can be rewritten into the form

$$\begin{aligned}\mathbf{J}^{T}\boldsymbol{F} + \mathbf{N}^{T}\boldsymbol{\tau} =& \mathbf{J}^{T}\mathbf{J}^{\#T}\left(\mathbf{H}\mathbf{J}^{\#}(\ddot{\boldsymbol{x}} - \dot{\mathbf{J}}\dot{\boldsymbol{q}}) + \mathbf{C}\dot{\boldsymbol{q}} + \boldsymbol{g} - \boldsymbol{\tau}_E\right) + \\ & \mathbf{N}^{T}\left(\mathbf{H}\mathbf{N}\ddot{\boldsymbol{q}} + (\mathbf{C}\dot{\boldsymbol{q}} + \boldsymbol{g}) - \boldsymbol{\tau}_E\right) + \\ & \left(\mathbf{J}^{T}\mathbf{J}^{\#T}\mathbf{H}\mathbf{N}\ddot{\boldsymbol{q}} + \mathbf{N}^{T}\mathbf{H}\mathbf{J}^{\#}(\ddot{\boldsymbol{x}} - \dot{\mathbf{J}}\dot{\boldsymbol{q}})\right)\end{aligned} \tag{10}$$

Note that the terms on the right side of the above equation are arranged into three groups. The first group includes the forces acting in the task space. The second group includes torques acting in the null space of $\mathbf{J}^T$. The third group represents the coupling forces and torques. To make the motion of the end-effector and the internal motion independent, it is necessary that the terms in the third group are always equal to zero

$$\mathbf{J}^{\#T}\mathbf{H}\mathbf{N} = \mathbf{N}^T\mathbf{H}\mathbf{J}^{\#} = \mathbf{0} \tag{11}$$

The only value of $\mathbf{J}^{\#}$ which satisfies the condition (11) is $\bar{\mathbf{J}}$ as defined in Eq. (8) [9, 5].

The equation of the end-effector motion subjected to generalized task forces $\boldsymbol{F}$ is given in the form [8]

$$\boldsymbol{F} = \mathbf{M}(\boldsymbol{q})\ddot{\boldsymbol{x}} + \boldsymbol{\mu}(\boldsymbol{q},\dot{\boldsymbol{q}}) + \boldsymbol{\gamma}(\boldsymbol{q}) - \boldsymbol{F}_E$$

where $\mathbf{M}$, $\boldsymbol{\mu}$, $\boldsymbol{\gamma}$ and $\boldsymbol{F}_E$ are, respectively, the $m\times m$ symmetric positive-definite matrix describing the inertial properties of the manipulator in the task space, the m-dimensional vector of Coriolis and centrifugal forces, the m-dimensional vector of gravity forces, and the m-dimensional vector of external forces, all acting in the task space

$$\mathbf{M} = \bar{\mathbf{J}}^T\mathbf{H}\bar{\mathbf{J}} = (\mathbf{J}\mathbf{H}^{-1}\mathbf{J}^T)^{-1}$$

$$\boldsymbol{\mu} = \bar{\mathbf{J}}^T\mathbf{C}\dot{\boldsymbol{q}} - \mathbf{M}\dot{\mathbf{J}}\dot{\boldsymbol{q}}, \quad \boldsymbol{\gamma} = \bar{\mathbf{J}}^T\boldsymbol{g}, \quad \boldsymbol{F}_E = \bar{\mathbf{J}}^T\boldsymbol{\tau}_E$$

The internal motion of the manipulator subjected to the torque applied through the null space of $\mathbf{J}^T$ can be obtained inserting the $\bar{\mathbf{J}}$ in Eq. 10.

$$\bar{\mathbf{N}}^T\boldsymbol{\tau} = \bar{\mathbf{N}}^T\mathbf{H}\bar{\mathbf{N}}\ddot{\boldsymbol{q}} + \bar{\mathbf{N}}^T(\mathbf{C}\dot{\boldsymbol{q}} + \boldsymbol{g}) - \bar{\mathbf{N}}^T\boldsymbol{\tau}_E$$

The matrix, which premultiplies $\ddot{\boldsymbol{q}}$ and is defined as

$$\mathbf{H}_n = \bar{\mathbf{N}}^T\mathbf{H}\bar{\mathbf{N}} = \mathbf{H} - \mathbf{J}^T\mathbf{M}\mathbf{J} \tag{12}$$

will be denoted as the *null space effective inertia matrix*. The matrix $\mathbf{H}_n$ describes the inertial properties of the system in the null space. As $\mathbf{H}_n$ has not a full rank, $\text{rank}(\mathbf{H}_n) < n$, we define the generalized inverse of the null space effective inertia matrix $\mathbf{H}_n$ as

$$\mathbf{H}_n^{\ddagger} = \bar{\mathbf{N}}\mathbf{H}^{-1}\bar{\mathbf{N}}^T$$

Note that $\mathbf{H}_n^{\ddagger}\mathbf{H}_n\mathbf{H}_n^{\ddagger} = \mathbf{H}_n^{\ddagger}$, $\mathbf{H}_n\mathbf{H}_n^{\ddagger}\mathbf{H}_n = \mathbf{H}_n$, and $\mathbf{H}_n^{\ddagger} = (\mathbf{H}_n^{\ddagger})^T$.

5. CONTROL ALGORITHMS

Most of the tasks performed by a redundant manipulator can be broken down into several subtasks with different priorities. In the following it is assumed that the subtask with the highest priority, referred to as the main task, is associated with the positioning of the end-effector and the force acting on the end-effector and the secondary task is to track a prescribed null space velocity.

Utilizing a formulation of the generalised forces a control law is given in the form

$$\boldsymbol{\tau} = \mathbf{J}^T\mathbf{M}(\ddot{\boldsymbol{x}}_c - \dot{\mathbf{J}}\dot{\boldsymbol{q}}) + \bar{\mathbf{N}}^T\mathbf{H}(\boldsymbol{\phi} + \bar{\mathbf{J}}\dot{\boldsymbol{x}}) + \mathbf{C}\dot{\boldsymbol{q}} + \boldsymbol{g} - \mathbf{J}^T\boldsymbol{F}_E \tag{13}$$

where $\ddot{\boldsymbol{x}}_c$ and $\boldsymbol{\phi}$ represent the control law for the task motion and internal motion, respectively and $\boldsymbol{F}_E$ is the task space force measured at the robot's tool centre point (TCP) using the force-torque sensor. The closed loop dynamics is obtained by inserting the above equation into Eq. 9.

$$\mathbf{H}\ddot{\boldsymbol{q}} - \boldsymbol{\tau}_E = \mathbf{J}^T\mathbf{M}(\ddot{\boldsymbol{x}}_c - \dot{\mathbf{J}}\dot{\boldsymbol{q}}) + \bar{\mathbf{N}}^T\mathbf{H}(\boldsymbol{\phi} + \bar{\mathbf{J}}\dot{\boldsymbol{x}}) - \mathbf{J}^T\boldsymbol{F}_E \tag{14}$$

Next, we will analyse the behaviour of the proposed controller in the task space and null space independently. Premultiplying Eq. 14 by $\mathbf{J}\mathbf{H}^{-1}$ and considering $\ddot{\boldsymbol{x}} = \mathbf{J}\ddot{\boldsymbol{q}} + \dot{\mathbf{J}}\dot{\boldsymbol{q}}$ we yields

$$\begin{aligned} \ddot{\boldsymbol{x}}_c - \ddot{\boldsymbol{x}} &= \mathbf{J}\mathbf{H}^{-1}(\mathbf{J}^T\boldsymbol{F}_E - \boldsymbol{\tau}_E) \\ &= -\mathbf{J}\mathbf{H}^{-1}\bar{\mathbf{N}}^T\boldsymbol{\tau}_E \\ &= 0 \end{aligned} \tag{15}$$

since $\mathbf{J}\mathbf{H}^{-1}\mathbf{J}^T\mathbf{M} = \mathbf{I}$ and $\mathbf{J}\mathbf{H}^{-1}\bar{\mathbf{N}}^T = 0$.

Similarly, null space dynamics can be obtained by premultiplying Eq. 14 with $\bar{\mathbf{N}}\mathbf{H}^{-1}$

$$\bar{\mathbf{N}}\ddot{\boldsymbol{q}} - \bar{\mathbf{N}}\mathbf{H}^{-1}\bar{\mathbf{N}}^T\boldsymbol{\tau}_E = \bar{\mathbf{N}}\mathbf{H}^{-1}\mathbf{J}^T\mathbf{M}(\ddot{\boldsymbol{x}}_c - \dot{\mathbf{J}}\boldsymbol{q}) + \bar{\mathbf{N}}\mathbf{H}^{-1}\bar{\mathbf{N}}^T\mathbf{H}(\boldsymbol{\phi} + \dot{\mathbf{J}}^{\#}\dot{\boldsymbol{x}}) \tag{16}$$

Considering that $\bar{\mathbf{N}}\mathbf{H}^{-1}\bar{\mathbf{N}}^T\mathbf{H} = \bar{\mathbf{N}}$ and $\bar{\mathbf{N}}\mathbf{H}^{-1}\mathbf{J}^T = 0$ we obtain

$$\bar{\mathbf{N}}(-\ddot{\boldsymbol{q}} + \boldsymbol{\phi} + \bar{\mathbf{J}}\dot{\boldsymbol{x}}) = -\mathbf{H}_n^{\ddagger}\boldsymbol{\tau}_E \tag{17}$$

5.1. Task space controller

Let $\ddot{\boldsymbol{x}}_c$ be selected as

$$\ddot{\boldsymbol{x}}_c = \ddot{\boldsymbol{x}}_d + \mathbf{K}_v\dot{\boldsymbol{e}} + \mathbf{K}_p\boldsymbol{e} + \mathbf{K}_f(\boldsymbol{F}_d - \boldsymbol{F}_E) \tag{18}$$

where $\boldsymbol{e}$, $\boldsymbol{e} = \boldsymbol{x}_d - \boldsymbol{x}$, is the tracking error, $\ddot{\boldsymbol{x}}_d$ is the desired task space acceleration, and $\mathbf{K}_v$, $\mathbf{K}_p$ and $\mathbf{K}_f$ are $n \times n$ constant gain matrices. The selection of $\mathbf{K}_v$, $\mathbf{K}_p$ and $\mathbf{K}_f$ can be based on the desired task space impedance. $\boldsymbol{F}_d$ denotes the desired external force. It is supposed that the external force $\boldsymbol{F}_E$ can be measured by an appropriate force/torque sensor. Substituting Eq. (18) for $\ddot{\boldsymbol{x}}_c$ in Eq. (15), yields

$$\ddot{\boldsymbol{e}} + \mathbf{K}_v \dot{\boldsymbol{e}} + \mathbf{K}_p \boldsymbol{e} = -\mathbf{K}_f (\boldsymbol{F}_d - \boldsymbol{F}_E)$$

As we can see the task space impedance can be chosen freely. By selecting $\mathbf{K}_v = \mathbf{M}_d^{-1}\mathbf{D}_d$, $\mathbf{K}_p = \mathbf{M}_d^{-1}\mathbf{K}_d$ and $\mathbf{K}_f^{"} = \mathbf{M}_d^{-1}\mathbf{K}_f$ the following task space impedance can be achieved

$$\mathbf{M}_d \ddot{\boldsymbol{e}} + \mathbf{D}_d \dot{\boldsymbol{e}} + \mathbf{K}_d \boldsymbol{e} = -\mathbf{K}_f^{"} (\boldsymbol{F}_d - \boldsymbol{F}_E)$$

$\mathbf{M}_d$, $\mathbf{D}_d$ and $\mathbf{K}_d$ are the desired task space inertia, damping and stiffness matrices, respectively.

5.2. Null space controller

Besides the main task, a redundant system can perform an additional subtask by selecting an appropriate vector $\boldsymbol{\phi}$ in the control law (13) which moves the manipulator toward the desired configuration. Let $\dot{\boldsymbol{\varphi}}_n$ be the desired null space velocity, $\dot{\boldsymbol{\varphi}}_n = \bar{\mathbf{N}}\dot{\boldsymbol{\varphi}}$. To obtain good tracking of $\dot{\boldsymbol{\varphi}}$ in the null space, the following $\boldsymbol{\phi}$ is proposed [15]

$$\boldsymbol{\phi} = \ddot{\boldsymbol{\varphi}}_n + k_n \dot{\boldsymbol{e}}_n + \mathbf{H}^{-1}\mathbf{C}\dot{\boldsymbol{e}}_n = \bar{\mathbf{N}}\ddot{\boldsymbol{\varphi}} + \bar{\mathbf{N}}\dot{\boldsymbol{\varphi}} + k_n \dot{\boldsymbol{e}}_n + \mathbf{H}^{-1}\mathbf{C}\dot{\boldsymbol{e}}_n \tag{19}$$

where $\dot{\boldsymbol{e}}_n = \bar{\mathbf{N}}(\dot{\boldsymbol{\varphi}} - \dot{\boldsymbol{q}})$ and k_n is positive scalar describing feedback gain.

Substituting (19) into (17) yields

$$\bar{\mathbf{N}}(\ddot{\boldsymbol{\varphi}} - \ddot{\boldsymbol{q}}) = \bar{\mathbf{N}}(-\mathbf{H}^{-1}\mathbf{C}\dot{\boldsymbol{e}}_n - k_n \dot{\boldsymbol{e}}_n - \bar{\mathbf{N}}\dot{\boldsymbol{\varphi}} - \bar{\mathbf{J}}\dot{\boldsymbol{x}}) - \mathbf{H}_n^{\ddagger}\boldsymbol{\tau}_E \tag{20}$$

Differentiating $\dot{\boldsymbol{e}}_n$ results in

$$\ddot{\boldsymbol{e}}_n = \bar{\mathbf{N}}(\ddot{\boldsymbol{\varphi}} - \ddot{\boldsymbol{q}}) + \bar{\mathbf{N}}(\dot{\boldsymbol{\varphi}} - \dot{\boldsymbol{q}}) \tag{21}$$

Using Eq. (20) in the above equation yields

$$\ddot{\boldsymbol{e}}_n = -\bar{\mathbf{N}}\mathbf{H}^{-1}\mathbf{C}\dot{\boldsymbol{e}}_n - \bar{\mathbf{N}}k_n \dot{\boldsymbol{e}}_n - \bar{\mathbf{N}}\dot{\boldsymbol{q}} - \bar{\mathbf{N}}\bar{\mathbf{J}}\dot{\boldsymbol{x}} - \mathbf{H}_n^{\ddagger}\boldsymbol{\tau}_E \tag{22}$$

Note that $\dot{\boldsymbol{\varphi}}$ belongs to the null space of $\mathbf{J}$ and $\bar{\mathbf{N}}\bar{\mathbf{J}}\dot{\boldsymbol{x}} = -\bar{\mathbf{N}}\bar{\mathbf{N}}\dot{\boldsymbol{q}}$. This can be verified by

$$\bar{\mathbf{N}}\bar{\mathbf{N}}\dot{\boldsymbol{q}} = -\bar{\mathbf{N}}(\dot{\bar{\mathbf{J}}}\mathbf{J} + \bar{\mathbf{J}}\dot{\mathbf{J}})\dot{\boldsymbol{q}} = -\bar{\mathbf{N}}\bar{\mathbf{J}}\dot{\boldsymbol{x}}$$

since $\bar{\mathbf{N}}\bar{\mathbf{J}} = 0$. Hence, Eq. (22) can be rewritten into the form

$$\ddot{\boldsymbol{e}}_n = -\bar{\mathbf{N}}k_n\dot{\boldsymbol{e}}_n - \bar{\mathbf{N}}\mathbf{H}^{-1}\mathbf{C}\dot{\boldsymbol{e}}_n - (\mathbf{I}-\bar{\mathbf{N}})\dot{\bar{\mathbf{N}}}\dot{\boldsymbol{q}} - \mathbf{H}_n^{\ddagger}\boldsymbol{\tau}_E \tag{23}$$

Next, we show that for $\mathbf{N}^T\boldsymbol{\tau}_E = 0$ the proposed control method (19) assures asymptotic stability of the system in the null space and that the $\dot{\boldsymbol{e}}$ converges to zero. In this case the last term $\mathbf{H}_n^{\ddagger}\boldsymbol{\tau}_E$ in Eq. 23 is equal to zero. Let the Lyapunov function be defined as $v = 1/2\ \dot{\boldsymbol{e}}_n^T\mathbf{H}\dot{\boldsymbol{e}}_n$. Differentiating v and substituting Eq. (23) for $\ddot{\boldsymbol{e}}$ yields

$$\begin{aligned}
\dot{v} =& \dot{\boldsymbol{e}}_n^T\mathbf{H}\ddot{\boldsymbol{e}}_n + \tfrac{1}{2}\dot{\boldsymbol{e}}_n^T\dot{\mathbf{H}}\dot{\boldsymbol{e}}_n \\
=& -\dot{\boldsymbol{e}}_n^T\mathbf{H}\bar{\mathbf{N}}k_n\dot{\boldsymbol{e}}_n - \dot{\boldsymbol{e}}_n^T\mathbf{H}\bar{\mathbf{N}}\mathbf{H}^{-1}\mathbf{C}\dot{\boldsymbol{e}}_n - \dot{\boldsymbol{e}}_n^T\mathbf{H}(\mathbf{I}-\bar{\mathbf{N}})\dot{\bar{\mathbf{N}}}\dot{\boldsymbol{q}} + \tfrac{1}{2}\dot{\boldsymbol{e}}_n^T\dot{\mathbf{H}}\dot{\boldsymbol{e}}_n \\
=& -\dot{\boldsymbol{e}}_n^T\mathbf{H}k_n\dot{\boldsymbol{e}}_n - \dot{\boldsymbol{e}}_n^T\mathbf{H}(\mathbf{I}-\bar{\mathbf{J}}\mathbf{J})\mathbf{H}^{-1}\mathbf{C}\dot{\boldsymbol{e}}_n - \dot{\boldsymbol{e}}_n^T\mathbf{H}(\bar{\mathbf{J}}\mathbf{J})\dot{\bar{\mathbf{N}}}\dot{\boldsymbol{q}} + \tfrac{1}{2}\dot{\boldsymbol{e}}_n^T\dot{\mathbf{H}}\dot{\boldsymbol{e}}_n \\
=& -k_n\dot{\boldsymbol{e}}_n^T\mathbf{H}\dot{\boldsymbol{e}}_n - \tfrac{1}{2}\dot{\boldsymbol{e}}_n^T(\dot{\mathbf{H}}-2\mathbf{C})\dot{\boldsymbol{e}}_n \\
=& -k_n\dot{\boldsymbol{e}}_n^T\mathbf{H}\dot{\boldsymbol{e}}_n
\end{aligned} \tag{24}$$

since $\dot{\boldsymbol{e}}_n^T\mathbf{H}\bar{\mathbf{J}} = 0$, $\bar{\mathbf{N}}\dot{\boldsymbol{e}}_n = \dot{\boldsymbol{e}}_n$ and $(\dot{\mathbf{H}}-2\mathbf{C})$ is skew symmetric [11]. Since v is positive definite and $\dot{v}$ is negative definite providing that k_n is positive scalar, $\dot{\boldsymbol{e}}_n$ tends to zero and the proposed controller stabilizes the null-space motion as long as the Jacobian is non-singular. Note that the matrix $(\dot{\mathbf{H}}-2\mathbf{C})$ is skew symmetric only if $\mathbf{C}(\boldsymbol{q},\dot{\boldsymbol{q}})$ is formed using Christoffel terms [11]. A similar result has been independently derived in [3]

Null space dynamics can be obtained from Eq. 23. First, we premultiply it with $\mathbf{H}_n$ and then use the Eq. 12

$$\begin{aligned}
\mathbf{H}_n\ddot{\boldsymbol{e}}_n =& -\bar{\mathbf{N}}^T\mathbf{H}\bar{\mathbf{N}}\bar{\mathbf{N}}k_n\dot{\boldsymbol{e}}_n - \bar{\mathbf{N}}^T\mathbf{H}\bar{\mathbf{N}}\bar{\mathbf{N}}\mathbf{H}^{-1}\mathbf{C}\dot{\boldsymbol{e}}_n \\
& -\bar{\mathbf{N}}^T\mathbf{H}\bar{\mathbf{N}}(\mathbf{I}-\bar{\mathbf{N}})\dot{\bar{\mathbf{N}}}\dot{\boldsymbol{q}} - \bar{\mathbf{N}}^T\mathbf{H}\bar{\mathbf{N}}\mathbf{H}_n^{\ddagger}\boldsymbol{\tau}_E
\end{aligned} \tag{25}$$

Since $\bar{\mathbf{N}}$ is idempotent, $\bar{\mathbf{N}}\bar{\mathbf{N}} = \bar{\mathbf{N}}$, it follows $\bar{\mathbf{N}}(\mathbf{I}-\bar{\mathbf{N}}) = 0$, $\mathbf{H}\bar{\mathbf{N}} = \bar{\mathbf{N}}^T\mathbf{H}$. Using the definition of $\mathbf{H}_n^{\ddagger}$, the equation 25 can be expressed in the form

$$\mathbf{H}_n\ddot{\boldsymbol{e}}_n + (\mathbf{H}_nk_n + \bar{\mathbf{N}}^T\mathbf{C})\dot{\boldsymbol{e}}_n = -\bar{\mathbf{N}}^T\boldsymbol{\tau}_E \tag{26}$$

The above equation describes the null space dynamics with the proposed control. Summarizing, the control method (19) enables to change the null-space damping by selecting k_n.

6. NULL SPACE MOTION OPTIMIZATION

The force and the position tracking are usually of the highest priority for a force controlled robot. The selection of the sub-tasks with lower priority depends on the specific application [4].

However, collision avoidance is of great importance, since the force controlled robot interacts with the environment. In our previous work we implemented obstacle avoidance algorithm using potential field. This approach requires the distance between the obstacle and any part of the robot. Beside being time consuming, this approach requires the at least approximate position of the environment obstacle. Here, we assume that this information is not known and can not be obtained. Therefore, we allow to the robot to bump into obstacles, but we try to minimize the resulting forces by adopting the null space dynamics.

An important sub-task for the force controlled robot might be to benefit the mechanical advantage of the manipulator in order to minimize joint torques when applying a certain force to the end effector. The local joint torque minimization as a performance objective was intensively investigated by many authors [6, 7, 2]. As the joint torque depends on the system dynamics it is difficult to express the gradient of the cost function related to joint torques. We simplified the problem by minimizing only joint torques related to the force applied to the robot end effector. We define the cost function in the form $\boldsymbol{p} = \boldsymbol{\tau}^T \boldsymbol{\tau}$, where $\boldsymbol{\tau} = \mathbf{J}^T \boldsymbol{F}_E$ is the joint torque due to the end effector force. Then, the cost function gradient required to minimize the given function can be expressed in the form

$$\frac{\partial \boldsymbol{p}}{\partial \boldsymbol{q}} = 2\boldsymbol{F}^T \mathbf{J} \nabla \boldsymbol{\tau}, \tag{27}$$

$$\nabla \boldsymbol{\tau} = \begin{bmatrix} \frac{\partial \mathbf{J}^{(1)}}{\partial \boldsymbol{q}_1}\boldsymbol{F} & \frac{\partial \mathbf{J}^{(1)}}{\partial \boldsymbol{q}_2}\boldsymbol{F} & \dots & \frac{\partial \mathbf{J}^{(1)}}{\partial \boldsymbol{q}_n}\boldsymbol{F} \\ \frac{\partial \mathbf{J}^{(2)}}{\partial \boldsymbol{q}_1}\boldsymbol{F} & \frac{\partial \mathbf{J}^{(2)}}{\partial \boldsymbol{q}_2}\boldsymbol{F} & \dots & \frac{\partial \mathbf{J}^{(2)}}{\partial \boldsymbol{q}_n}\boldsymbol{F} \\ \vdots & \vdots & \vdots & \vdots \\ \frac{\partial \mathbf{J}^{(n)}}{\partial \boldsymbol{q}_1}\boldsymbol{F} & \frac{\partial \mathbf{J}^{(n)}}{\partial \boldsymbol{q}_2}\boldsymbol{F} & \dots & \frac{\partial \mathbf{J}^{(n)}}{\partial \boldsymbol{q}_n}\boldsymbol{F} \end{bmatrix}, \tag{28}$$

where $\mathbf{J}^{(i)}$ denotes the i-th column of the Jacobian $\mathbf{J}$. This approach can be justified by the fact that velocities and acceleration during the force tracking are usually low. Another advantage using this approach is that the minimization can be related to the desired end-effector force and the manipulator can be brought to the optimal pose before the contact with the environment is established.

The desired null space velocities can be obtained utilizing modified gradient optimization procedure

$$\dot{\varphi} = \bar{\mathbf{J}}\dot{\boldsymbol{x}} + \bar{\mathbf{N}} k_o \mathbf{H}^{-1} \psi, \tag{29}$$

which assures the best optimization step in the case of inertia weighted pseudo-inverse. k_o

defines the optimization step. Vector ψ is a gradient optimization vector defined as

$$\psi = (\frac{\partial \boldsymbol{p}}{\partial q_1}, \frac{\partial \boldsymbol{p}}{\partial q_2}, ..., \frac{\partial \boldsymbol{p}}{\partial q_N})^T \tag{30}$$

Unfortunately, the local joint torque minimization often brings the robot into the singular configuration. Therefore, the singularity avoidance algorithm also has to be implemented. We have accomplished this task by maximizing manipulator manipulability proposed by [18].

7. EXPERIMETS

In this section, we show the performance of the proposed control strategy on simulation and experimental result on 4 d.o.f planar redundant manipulator.

7.1. System Description

The experimental setup consists of 4-DOF planar redundant robot with all segments of equal length $0.25m$, presented in Fig. 1. The robot had no limits in joint angles. All AC brushless motors were located in the robot base in order to obtain lightweight links. The robot gear ratio was 6, thus the coupled dynamics of the robot was not negligible. We used two JR3 force sensors, capable of measuring three forces and three torques. One sensor was used for force tracking and the other for measuring contact force with an obstacle. The sensor used for force tracking was too heavy to be carried by the experimental robot, therefore we mounted the sensor under the environment plane. The obstacle was a vertical bar mounted on the force sensor. Forces from this sensor were used to measure the contact forces between the robot and the obstacle. The robot controller consists of a Pentium II 360 MHz industrial computer. The proposed control algorithm was realized on SIMULINK and compiled using Simulink Real Time Workshop and Planar Manipulator Toolbox.

[Figure 1 about here.]

7.2. Experimental results

The primary task of the manipulator was to track the desired force while moving along the wall in horizontal (x) direction. The desired speed was $0.45m/s$ and the desired force was $10N$. There was an obstacle in the robot work-space, as shown in Fig. 5. The position of the

obstacle and the contact forces were not known in the control law. The secondary subtasks were minimization of contact forces, minimization of the joint torques due to the end-effector force and maximization of the manipulability index. Because the impact was not the issue, we started the experiment with the robot in contact with the wall.

First, we have tested the proposed control law using the simulation. The simulation results of position tracking, force tracking and obstacle force are presented in Fig. 2, 3 and 4 respectively. Fig 5 shows poses of the robot in subsequent time intervals. From the results we can see that the obstacle contact forces had virtually no influence on the primary task, which was force and trajectory tracking. By selecting the appropriate null space dynamics, contact forces were minimized.

[Figure 2 about here.]

[Figure 3 about here.]

[Figure 4 about here.]

[Figure 5 about here.]

We repeated the same task on the real robot. We obtained control rate of 500 Hz. The results are presented in Figs. 6, 7 and 8. In this case we can notice the influence of the contact force with the obstacle to the TCP tracking error and TCP force. The performance degradation is manly due to the elasticity of the gear belts and gear friction. Although we included nonlinear friction compensator into the control loop, it was not possible to cancel the friction effect.

[Figure 6 about here.]

[Figure 7 about here.]

[Figure 8 about here.]

8. CONCLUSION

The paper considers the force control of redundant robots in presence of unknown obstacles. Instead of an obstacle avoidance algorithm we have changed the dynamics properties of the redundant manipulator in order to minimize the impact forces. Therefore, special attention is given to the dynamic decoupling and the inertial properties of the system in the space where internal motion is taking place; we define a *null space effective inertia* and its inverse. Finally, we propose a control algorithm (13) which decouples the motion of the manipulator into the end-effector motion and the internal motion. The controller enables the selection of dynamic characteristics in both subspaces separately. The proposed algorithm was tested using the simulation and on the real robot. With the simulation results we show that we have successfully decoupled null space and task space dynamics. Disturbance, caused by the obstacle, has virtually no effect on the primary task. Experiments on the real robot show similar results, but the performance is degraded by the elasticity and the friction in the robot joints. On the other hand, compliant dynamics requires low null space gains, which limits the performance of the null space tracking algorithm.

REFERENCES

[1] H. Asada and J.-J. Slotine. *Robot Analysis and Control*. John Wiley & Sons, 1986.

[2] T. Chen, F. Cheng, Y. Sun, and M. Hung. Torque optimization schemes for kinematically redundant manipulators. *J. of Robotic Systems*, 11(4), 1994.

[3] C.NAtale, B. Siciliano, and L. Vilani. Spatial impedance control of redundant manipulators. In *Proc. IEEE Int. Symp. on Robotics and Automation ICRA'99*, Detroit, 1999.

[4] R. Dubey and J. Luh. Redundant Robot Control Using Task Based Performance Measures. *J. of Robotic Systems*, 5(5):409 – 432, 1988.

[5] R. Featherstone and O. Khatib. Load Independance of the Dynamically Consistent Inverse of the Jacobian Matrix. *Int. J. of Robotic Research*, 16(2):168 – 170, 1997.

[6] J. M. Hollerbach and K. C. Suh. Redundancy resolution of manipulators through torque optimization. *IEEE Trans. on Robotics and Automation*, RA-3(4):308 – 316, 1987.

[7] H. Kang and R. Freeman. Null space damping method for local joint torque optimization of redundant manipulators. *J. of Robotic Systems*, 10(2):249 – 270, 1993.

[8] O. Khatib. A unified approach for motion and force control of robot manipulators:the operational space formulation. *IEEE Trans. on Robotics and Automation*, 3(1):43 – 53, 1987.

[9] O. Khatib. The Impact of Redundancy on the Dynamic Performance of Robots. *Laboratory Robotics and Automation*, 8(1):37 – 48, 1996.

[10] C. A. Klein and C. H. Huang. Review of pseudoinverse control for use with kinematically redundant manipulators. *IEEE Trans. on Systems, Man, Cybernetics*, SMC-13(3):245 – 250, 1983.

[11] B. S. L. Sciavicco. *Modelling and Control of Robot Manipulators*. McGraw-Hill, New York, 1996.

[12] J. Luh. Convetional controller design for industrial robots — a tutorial. *IEEE Trans. on Systems, Man, Cybernetics*, SMC-13(3):298 – 316, 1983.

[13] J. Luh, M. Walker, and R. Paul. Resolved acceleration control of mechanical manipulators. *IEEE Trans. on Automati Control*, AC-25(3):486 – 474, June 1980.

[14] A. Maciejewski. Kinetic limitations on the use of redundancy in robotic manipulators. *IEEE Trans. on Robotics and Automation*, 7(2):205 – 201, 1991.

[15] B. Nemec and L. Žlajpah. Experiments on impedance control of redundant manipulators. In *Proc. IEEE Int. Symp. on Industrial Electronics ISIE'99*, pages 134–138, Bled, 1999.

[16] D. N. Nenchev. Redundancy resolution through local optimization: A review. *J. of Robotic Systems*, 6(6):769 – 798, 1989.

[17] J. Park, W. Chung, and Y. Youm. Weighted Decomposition of Kinematics and Dynamics of Kinematically Redundant Manipulators. In *Proc. IEEE Conf. Robotics and Automation*, pages 480 – 486, 1996.

[18] T. Yoshikawa. *Foundations of robotics: analysis and control*. MIT Press, 1990.

List of Figures

[Figure 9 about here.]

[Figure 10 about here.]

[Figure 11 about here.]

[Figure 12 about here.]

[Figure 13 about here.]

[Figure 14 about here.]

[Figure 15 about here.]

[Figure 16 about here.]

List of Figures

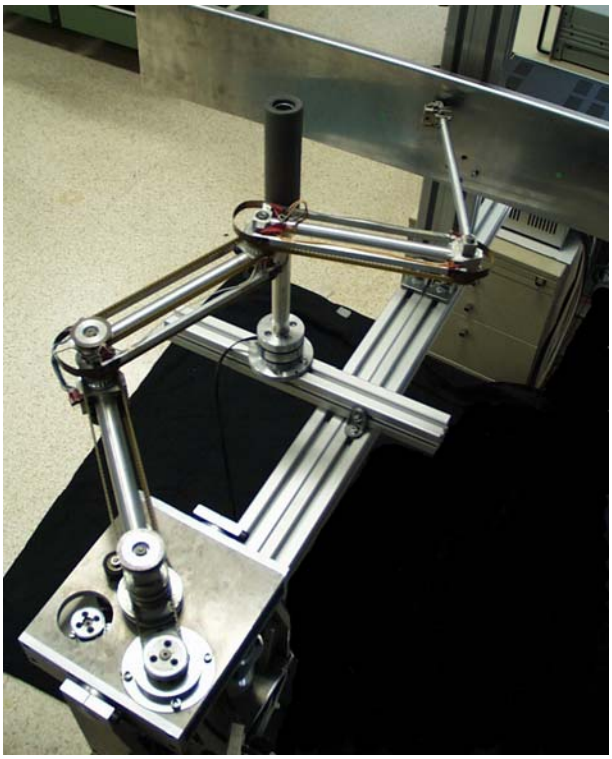

Figure 1: 4-D.O.F experimental robot

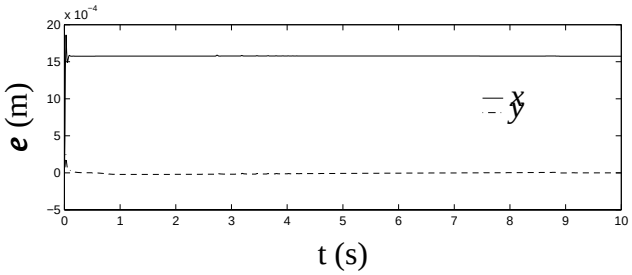

Figure 2: Simulated TCP tracking error

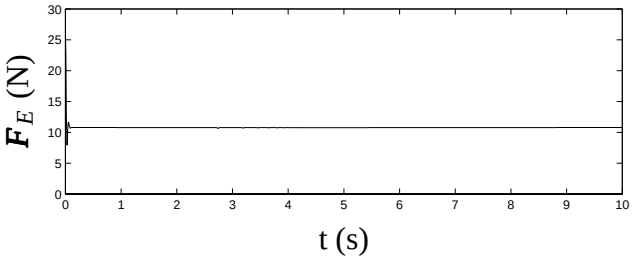

Figure 3: Simulated TCP force

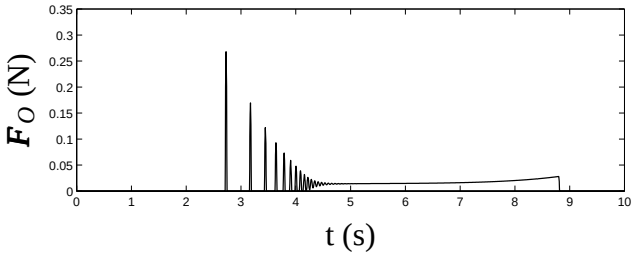

Figure 4: Simulated obstacle force

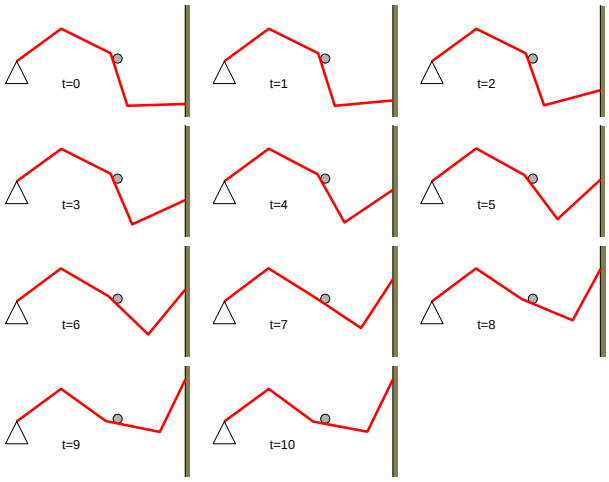

Figure 5: Poses of the robot during the simulation of the task

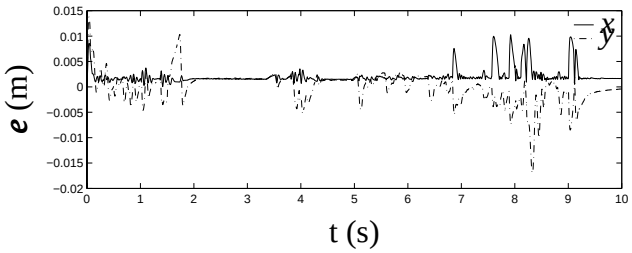

Figure 6: TCP tracking error

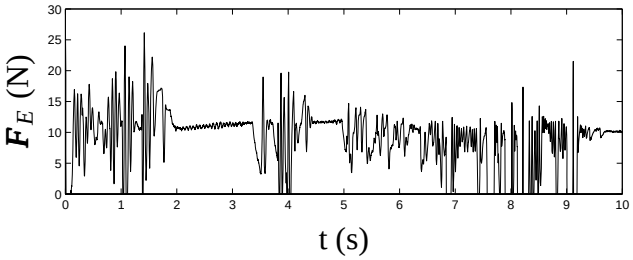

Figure 7: TCP force

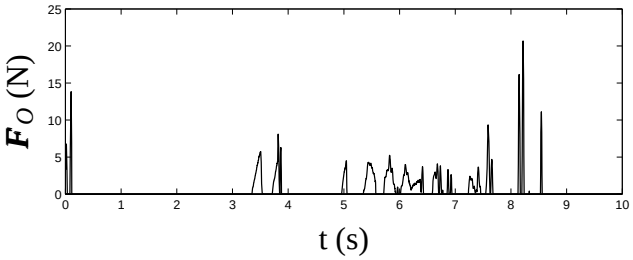

Figure 8: Obstacle force

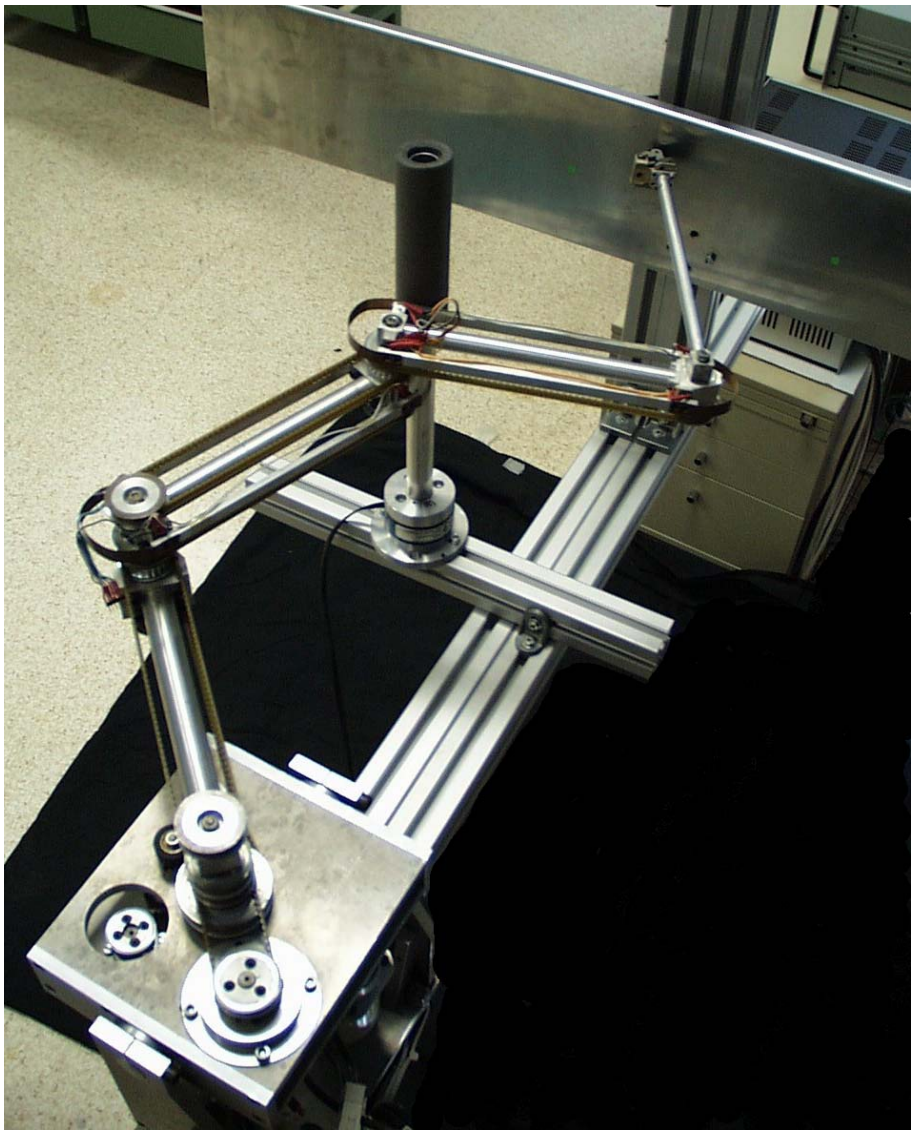

Figure 9: 4-D.O.F experimental robot

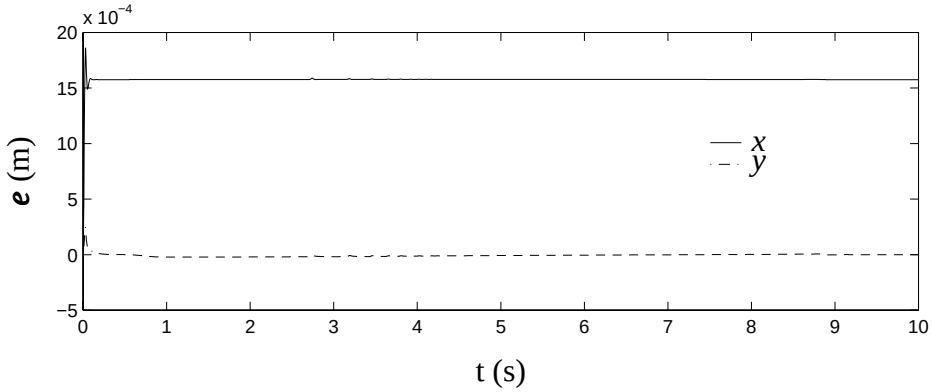

Figure 10: Simulated TCP tracking error

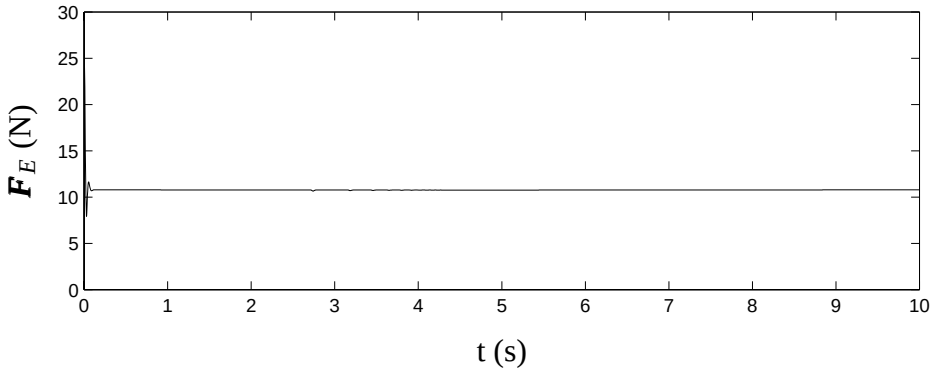

Figure 11: Simulated TCP force

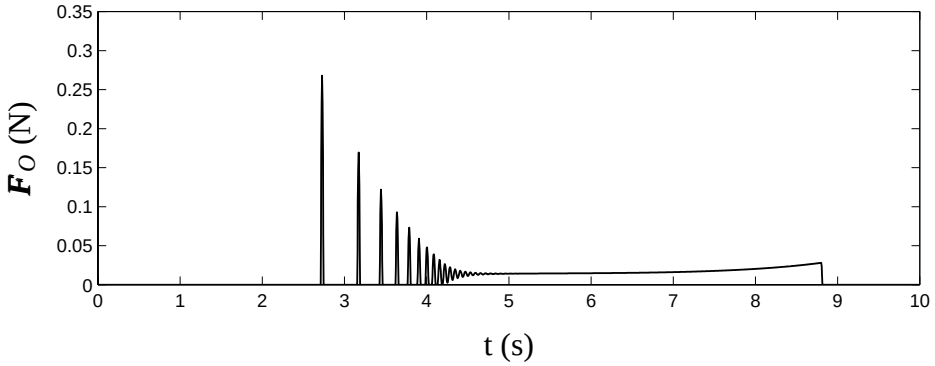

Figure 12: Simulated obstacle force

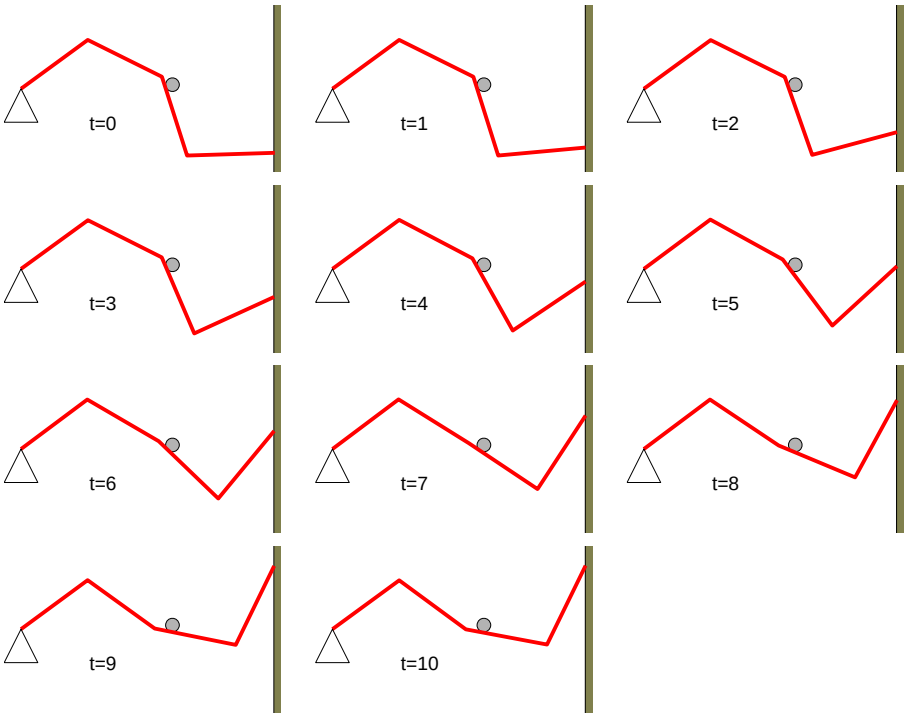

Figure 13: Poses of the robot during the simulation of the task

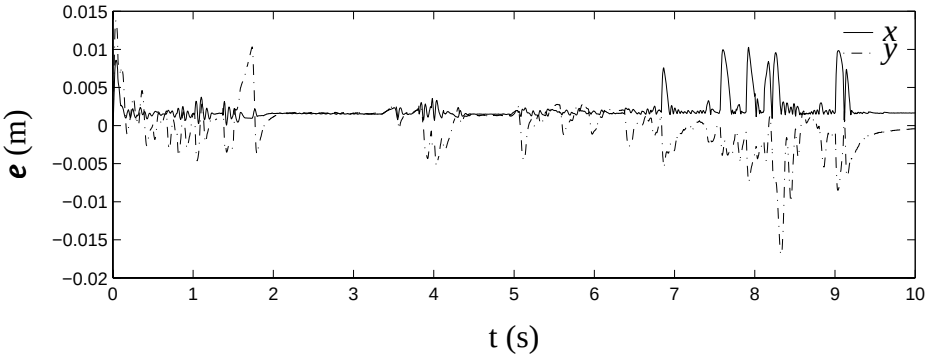

Figure 14: TCP tracking error

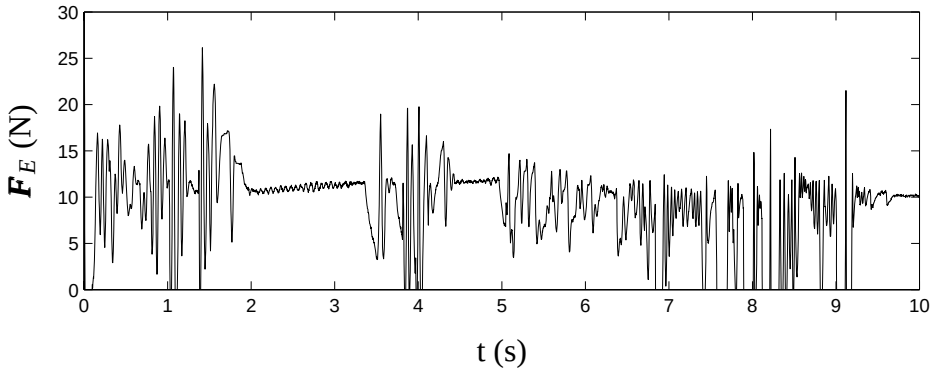

Figure 15: TCP force

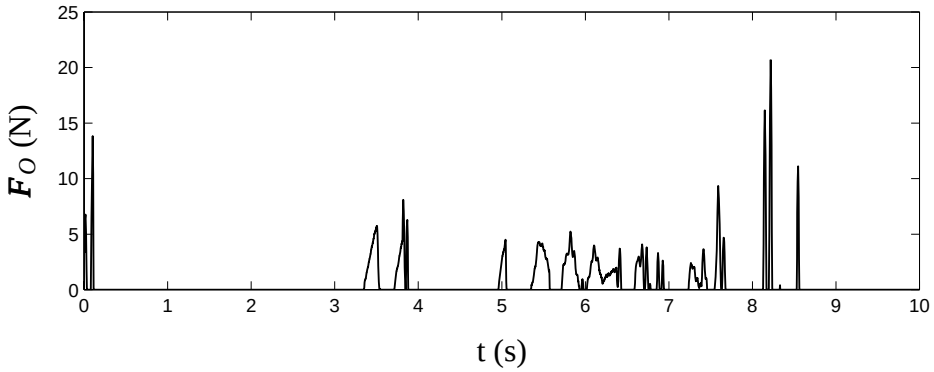

Figure 16: Obstacle force